# An Equation of State Tabulation Approach for Injectors with Non-Condensable Gases: Development and Analysis

Mathis Bode[a,*], Sutharsan Satcunanathan[b], Kazuki Maeda[c], Tim Colonius[d], Heinz Pitsch[a]

[a] *Institute for Combustion Technology, RWTH Aachen University, 52056 Aachen, Germany*
[b] *Institute for Aerodynamics, RWTH Aachen University, 52056 Aachen, Germany*
[c] *Mechanical Engineering, University of Washington, Seattle, WA 98195, USA*
[d] *Department of Mechanical Engineering, California Institute of Technology, Pasadena, CA 91125, USA*

## Abstract

In this work, a general equation of state (EOS) tabulation method is presented, which allows arbitrary combinations of EOSs in different phases and can be used with single-phase flow solvers by adding one additional transport equation for the total partial density of all non-condensable gases. The new tabulation method assumes instantaneous equilibrium for all phase change processes and uses Legendre transformation to construct the convex hull of the energy surface. Newton iterations are applied to improve the accuracy within the tabulation step as well as of the data retrieved at runtime. A high-order 5-equation multiphase solver with stiffened-gas equations as EOS for all phases and with the ability to use different time scales for the relaxation processes between liquid and vapor phase is used to discuss the full equilibrium assumption of the tabulation approach. Furthermore, results using different EOSs for the tabulation are compared. The implication of choosing a stiffened-gas equation or a cubic EOS, such as the Peng-Robinson equation for the vapor phase, on the saturation quantities is discussed. A nozzle simulation performed under typical gasoline direct injection (GDI) conditions is finally used to demonstrate the advantages of the new tabulation method and to evaluate additional computational cost.

**Keywords:** Equation of State; Homogeneous Equilibrium Model; Cavitation; Non-Condensable Gases; Injector Flows; Homogeneous Relaxation Model

## Introduction

The performance of direct injection engines strongly depends on the injection process of the liquid fuel. This process is influenced by phase change, including cavitation inside the nozzle. For an accurate prediction of the nozzle flow, non-condensable gases have been found to be important, resulting in a flow configuration with three different phases: liquid fuel, fuel vaporl, and non-condensable gases [1, 2]. Small amounts of non-condensable gases are typically dissolved in the liquid fuel, but they can also penetrate into the nozzle from the low-pressure chamber. This phenomenon is known as hydraulic flip.

For the described multiphase systems, $N$-equation models have become popular in recent years [3, 4, 5, 6, 7, 8]. The so-called 7-equation model, which yields conservation equations for mass, momentum, and energy for a liquid and a gas phase as well as an additional gas volume fraction transport equation, has been successfully reduced to 6-, 5-, and 4-equation systems by assuming kinetic, mechanic, and thermodynamic equilibrium. Also, extensions to more than two phases and systems with phase change have been presented. However, the application of these models is both expensive due to the additional equations and complex due to the requirement of additional boundary conditions compared to single-phase solvers. Also the closure of the extra source terms, for example in the context of large-eddy simulations (LESs), is unsolved.

Due to their flexibility and simple utilization in flow solvers originally designed for single-phase flows, equation of state (EOS) tabulation methods are an alternative approach. However, for nozzle flows, existing tabulation methods suffer from one of the following issues: Either they cannot account for non-condensable gases or they are unable to

*Corresponding Author, Mathis Bode: m.bode@itv.rwth-aachen.de

use different analytical EOSs for liquid fuel and fuel vapor, which is important for accurately predicting both fuel phases and phase changes simultaneously. This is adressed in this work by developing and analyzing a 3-equation homogeneous equilibrium model (HEM) for 3-phase systems. It emerges from the 7-equation model by assuming kinematic, mechanic, thermodynamic, and chemical equilibrium and requires only the solution of the well-known single-phase Navier-Stokes equations. The complexity of the model is hidden in the construction of a convex EOS that covers multiple phases. Since Maxwell constructions are not able to deal with arbitrary EOSs [9], Legendre transformation (LT) is used to construct the convex hull of the energy surface and recover convexity [10]. This is crucial for a wide validity of the model. The resulting thermodynamic properties are tabulated and a subsequent table lookup method is employed for incorporation of the HEM into a 3-equation flow solver. The accuracy of both, the tabulation step and the data retrieved, is improved by Newton iterations.

## 3-Phase Homogeneous Equilibrium Model

The EOS alters the flow equations through the flux function. In pure phases, these are known to be smooth convex functions. When phase transfer effects are included in the EOS, the flux function becomes non-smooth allowing new wave structures. A single EOS that attempts to cover the pure liquid, the pure vapor, the pure gas, and the mixture region exhibits a non-physical region of negative speed of sound, where convexity constraints from the 2$^{\text{nd}}$ law of thermodynamics are violated. Thus, the construction of a convex, i. e. thermodynamically admissible, equilibrium EOS out of convex single-fluid EOSs is one main challenge for tabulated EOS of 3-phase systems. One way to achieve the convexification is by strictly enforcing the equilibrium conditions. Denoting liquid by the subscript 'l', the corresponding vapor by 'v', the consolidation of all non-condensable gases by 'o', and mass fractions by $Y$, these can be summarized as

| | | |
|---|---|---|
| Temperature equilibrium ($T$) | $T = T_\mathrm{l} = T_\mathrm{v} = T_\mathrm{o}$ | (1a) |
| Pressure equilibrium ($p$) | $p_\mathrm{l} = p_\mathrm{v} + p_\mathrm{o}$ | (1b) |
| Chemical equilibrium ($\mu$) | $\mu_\mathrm{l} = \mu_\mathrm{v}$ | (1c) |
| Specific volume ($v$) | $v = (1 - Y_\mathrm{o} - Y_\mathrm{v})v_\mathrm{l} + Y_\mathrm{v} v_\mathrm{v}$ | (1d) |
| Specific internal energy ($e$) | $e = (1 - Y_\mathrm{o} - Y_\mathrm{v})e_\mathrm{l} + Y_\mathrm{v} e_\mathrm{v} + Y_\mathrm{o} e_\mathrm{o}$ | (1e) |
| Miscibility condition | $v_\mathrm{v} Y_\mathrm{v} = v_\mathrm{o} Y_\mathrm{o}$ | (1f) |

Alternatively, the convexification can be done by means of LT. Due to the higher flexibility, LT is used for this work as explained in the next subsection.
Besides the thermodynamic validity of the 3-phase HEM, accuracy is an important property of the model. This is especially true for the mixture region, where strong gradients occur across the phase boundaries. The developed HEM allows to flexibly combine exact, analytical expressions in the pure fluid regions and looked up values in the mixture region, which can be improved by Newton iterations on runtime using tabulated initial values and locally converging optimized Newton schemes. This hybrid combination allows high accuracy at moderate computational cost with a maximum of flexibility. Details are given in Subsection 'Hybrid Approach'.

### *Convexification*

In this work, LT is used for the convexification and is denoted for any function $\tilde{f}$ as

$$\tilde{f}^* : \xi \in \mathbb{R}^n \to \mathbb{R}; \xi \mapsto \sup_{x \in \mathbb{R}^n} \left\{ \langle \xi, x \rangle - \tilde{f}(x) \right\} \tag{2}$$

with $\langle \cdot, \cdot \rangle$ as scalar product on $\mathbb{R}^n$. Applying LT twice results in the biconjugate $\tilde{f}^{**}$, which is in general the convex hull of $\tilde{f}$. The construction of the convex hull of the energy surface is complicated by the non-intuitive set of variables $v, s, e$ (with $s$ as entropy) given by the fundamental relations [10], since it makes the choice of an appropriate domain for the LT difficult. Especially the edges of the domain might be located in regions, where the respective EOS loses its validity, leading to steep gradients, which have major impact on the dual space since $\xi \propto \nabla e$. This was further emphasized by computations, which have shown that the choice of the dual sets $\Omega_{\xi v}$ and $\Omega_{\xi s}$ is crucial for the

accuracy of the resulting table. If the dual set is chosen to be equally spaced between $\min(\xi_i)$ and $\max(\xi_i)$, this might distort the physically interesting regions by decreasing the resolution. To overcome these problems in this work, the easier measurable quantities temperature and pressure are used to cluster grid points in regions of interest, which is possible due to $(\xi^v, \xi^s)^T \propto \nabla e(v,s) = (-p, T)^T$. I. e. the negative of the pressure is dual to specific volume and temperature is dual to entropy. Consequently, the EOS-table is built as follows: Given a temperature and pressure range $\Omega_{T,p} = [T_{\min}, T_{\max}] \times [p_{\min}, p_{\max}]$, the sets $\Omega_{\xi^v}$ and $\Omega_{\xi^s}$ are chosen such that

$$n_{T,\text{rel}} = \left\{ |\Omega^T_{\xi^v}| / |\Omega_{\xi^v}| \mid T_{\min} \leq \xi^v_i \leq T_{\max}, \forall \xi^v_i \in \Omega^T_{\xi^v}, \Omega^T_{\xi^v} \subseteq \Omega_{\xi^v} \right\} \tag{3}$$

and

$$n_{p,\text{rel}} = \left\{ |\Omega^p_{\xi^s}| / |\Omega_{\xi^s}| \mid -p_{\max} \leq \xi^s_i \leq -p_{\min}, \forall \xi^s_i \in \Omega^p_{\xi^s}, \Omega^p_{\xi^s} \subseteq \Omega_{\xi^s} \right\} \tag{4}$$

are greater than some prescribed values and $\xi^v_1 \leq \min_j \xi^{v,j}_1$, $\xi^v_{N_{\xi^v}} \geq \max_j \xi^{v,j}_{N_{\xi^v}}$ and $\xi^s_1 \leq \min_i \xi^{s,i}_1$, $\xi^s_{N_{\xi^s}} \geq \max_i \xi^{s,i}_{N_{\xi^s}}$ with $n$ as number of points for the specified dimension for the tabulation. The superscripts $j$ and $i$ indicate their belonging to the sets $\Omega^j_{\xi^v}$ and $\Omega^i_{\xi^v}$ and the latter condition ensures that the domain of $e^{**}$ matches with that of $e$. Consequently, in total $n_{T,\text{rel}} \cdot n_{p,\text{rel}}$ of the points will be located in $\Omega_{T,p}$. This can even be improved, if the distribution density of the slopes additionally enters the determination of the dual sets, which is done in this work. Furthermore, to account for the stiff liquid phase it is crucial to have high resolution for small $v$ to capture the steep gradients. Therefore, a logarithmic scale for the $v$-axis is chosen, while the $s$-axis is kept linear during tabulation.

*Hybrid Approach*

The physics of 3-phase systems considerably differs from 2-phase systems. For example, due to the Gibbs' phase rule, which gives degrees-of-freedom $\hat{f} = 2$, the well-known thermodynamic characteristics of phase equilibrium ($v_{\text{l,sat}}(v_{\text{v,sat}})$, $T_{\text{sat}}(v_{\text{v,sat}})$, $p_{\text{sat}}(v_{\text{v,sat}})$, ... with 'sat' denoting saturation) cannot be employed and $v_{\text{v,sat}}$ is not suited to parametrize the boundary of the mixture region, although it is most suited for 2-phase systems [9]. The isotherms in the $p$-$v$-space are no longer horizontal lines and the phase boundary is not a 1D set of points.

System 1 summarizes the equilibrium conditions for 3-phase systems, which are the starting point of the HEM. It can be seen that for computing the thermodynamic state for given $v$, $e$, and $Y_{\text{o}}$, iterating on $v_{\text{v}}$ and $T$ circumvents the necessity to solve implicit relations. Since this set of nonlinear equations cannot be solved explicitly, Newton iteration methods are used. More than one possible combination of two equations, on which to perform the iteration, exists where condition Equation 1a is implicitly enforced by using one global temperature $T$ and therefore drops out. There still remain $(4-1)! = 6$ combinations, when the miscibility condition is not included. It has been observed that the choice of the Newton scheme (NS) for NS$[p, \mu]$, NS$[v, e]$, and NS$[p, e]$ strongly affects the convergence for different regions in the $v$-$e$-$Y_{\text{o}}$-space and thus the performance of the tabulation method. Therefore, the optimal choice has been also precomputed for this work and stored as part of the EOS-table in order to save computational cost. Furthermore, the domain of convergence was extended by dynamically adapting the relaxation parameter of the Newton iteration based on physical considerations. This was found to be especially important for very low volume fractions of the non-condensable gases, where the system of equations is ill-conditioned since the physics changes considerably from 3-phase to 2-phase systems rendering the system very stiff.

## Results and Discussion

*Comparison of Stiffened-Gas/Stiffened-Gas with Stiffened-Gas/Peng-Robinson*

The choice of the EOSs of the different phases in a multiphase simulation is crucial. It is well-known that cubic EOS such as the Peng-Robinson EOS (PR-EOS) have problems to accurately represent liquids due to their small compressibility. This combined with the simple usage of stiffened-gas EOSs (SG-EOSs) and the limited possibility of combining arbitrary EOSs have made the usage of SG-EOSs for both the liquid and the vapor phase popular. The developed HEM allows to study the accuracy of various EOS combinations. For that, EOS coefficients were fitted [11, 12] and compared to experimental data from the National Institute of Standards Technology (NIST) database. The comparison is shown in Figure 1. The liquid parameters are not influenced by the coupled vapor EOS and only the slightly different equilibrium states result in negligible differences for the saturated liquid quantities. Thus, all

EOS combinations with SG-EOS for the liquid phase share almost the same graph and for the sake of readability only one representative graph labeled 'SG' is plotted. The plots cover a fairly large temperature range nearly up to the critical point. Since SG-EOS does not support this point, 'SG/PR' does not give meaningful results when approaching the critical point either. For $p_{\mathrm{sat}}$, $L_{\mathrm{v}}$ and all vapor quantities except for the speed of sound, 'SG/SG' shows good agreement within a limited temperature range, but then starts to gradually deviate from the experimental curves for higher temperatures. Overall, the quality of the fit for SG-EOS depends strongly on the chosen temperature interval for the parameter determination. The saturated liquid speed of sound reveals one main shortcoming of SG-EOS, which is that complex molecular interactions are neglected. Even the monotonicity is miss-predicted. This can be ascribed to the expression for the speed of sound, which is a pure function of the temperature with $\frac{\partial c^2}{\partial T} = C_{\mathrm{v}}\gamma(\gamma - 1) > 0$ (with $c$ as speed of sound, $C_{\mathrm{v}}$ as specific heat capacity at constant volume, and $\gamma$ as heat capacity ratio) and thus unable to predict the tendency of decreasing speed of sound with temperature.

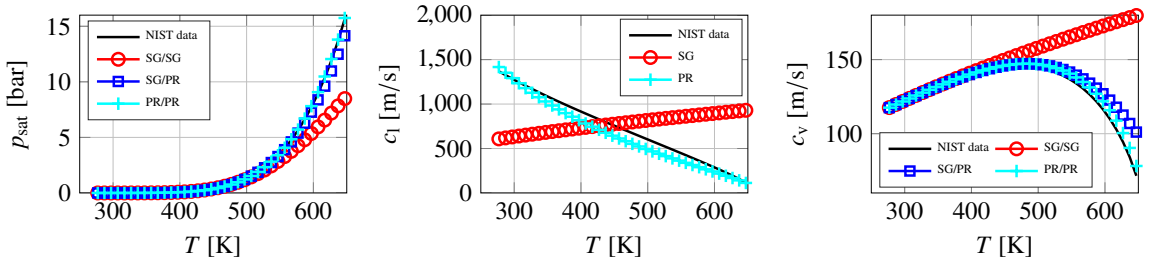


(a) Saturation pressure (b) Liquid sound speed (c) Vapor sound speed

Figure 1: Dodecane at saturation in the temperature interval $T = [273\,\mathrm{K}, 647\,\mathrm{K}]$.

*1D Validation*

To evaluate the 3-equation HEM for multiphase applications, a two-phase shock tube ($Y_{\mathrm{o}} = 0$) with dodecane and the conditions proposed by Saurel et al. [3] was computed. For a better comparability with other $N$-equtation models, SG-EOS is used for both phases and the results are compared to results computed with a 5-equation model with complete relaxation [8]. Due to different model assumptions, two points needs to be kept in mind during the analysis: First, according to Gibbs' phase rule, each pure phase in the mixture is determined by one state variable and exactly one combination of $T, p$ in the initial conditions (ICs) will allow the system to be in a mixture equilibrium state. In contrast, in the relaxation models, phase transfer can be dynamically controlled, for instance to suppress phase transfer at metastable states. Consequently, these models can handle non-equilibrium ICs and the developed HEM cannot. Second, even in pure phase regions, a small fraction of the respective other (actually non-present) phase is usually included in $N$-equation model simulations for numerical reasons. The proposed model is able to deal with real pure phases without a need for a lower threshold.

In Figure 2, the results at $t = 0.473\,\mathrm{ms}$ are compared to those of the 5-equation model with infinite relaxation and the same ICs, number of cells, and CFL number. From left to right, an expansion wave in the pure liquid, a contact discontinuity separating the liquid-vapor mixture from the pure vapor, and a shock in the pure vapor can be seen. The pressure plateau belongs to the state at the phase boundary with $p_{\mathrm{sat}}(T = 606\,\mathrm{K}) = 11.7\,\mathrm{bar}$, where the isentrope exhibits a kink, resulting in a discontinuity in the speed of sound. This leads to the observed wave splitting into the fast-running expansion wave in the pure liquid followed by the continuation of the expansion in the mixture region by the low speed wave, propagating with the mixture speed of sound. The left-running expansion wave (including the evaporation front) propagates with the wave speed of the acoustic mode $u - c$. The speed of sound of the 3-equation model over the length of the tube is depicted in Figure 2c. It has two discontinuities corresponding to the saturated liquid at $x \approx 0.21\,\mathrm{m}$ and saturated vapor at the contact discontinuity.

The results of both models perfectly coincide and also agree with data in the literature [3, 5, 7]. All wave velocities have been predicted equally. This concludes that the wave structure of the 5-equation model with full relaxation (i. e. including stiff source terms) corresponds to that of the 3-equation equilibrium model. That is, by full relaxation in the

mixture region, the consequences on the expansion wave coming from the discontinuity of the speed of sound in the 3-equation model, but missing in the 5-equation model, are restored.

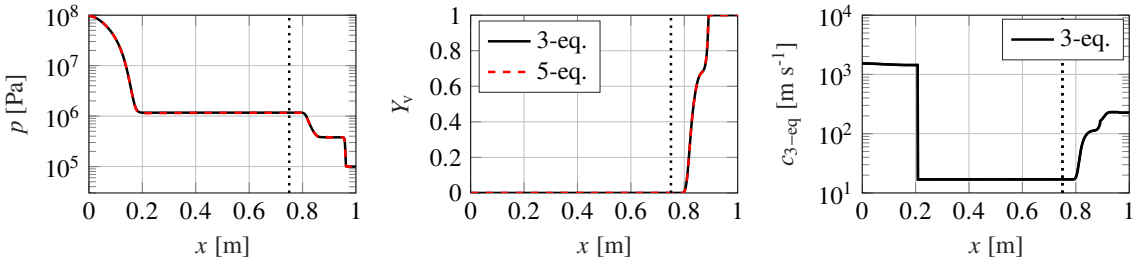


(a) Pressure (b) Vapor mass fraction (c) Speed of sound

Figure 2: Dodecane liquid-vapor shock tube results at $t = 0.473$ ms. The location of the initial discontinuity is highlighted by a dotted line. The number of cells is 1200 and the time step was specified by CFL = 0 .5. Comparison between the 3-equation HEM and the 5-equation model with infinite relaxation (two left plots) shows perfect agreement. The speed of sound of the 3-equation model exhibits two discontinuities, namely at the right end of the rarefaction wave and at the contact discontinuity (right plot).

*2D Model Evaluation*

The key assumption of the developed 3-equation HEM is that full equilibrium is reached infinitely fast. An alternative approach is represented by so-called homogeneous relaxation models (HRM) [13]. They were implemented in the context of an Eulerian mixture model by Schmidt et al. [14] for simulations of cavitating nozzle flows in order to include non-equilibrium effects by introducing a time scale $\theta_0$, at which the local vapor mass fraction relaxes towards its equilibrium value based on an empirical correlation, which was fitted for water. A comparison of results from the HRM to experimental results from X-ray imaging showed good agreement [15]. However, the evaluation of the time scales is completely empirical and difficult because typically no experiments for real fuels exist. The impact of different choices of the relaxation time scale in terms of $\theta_0$ for the shock tube case considered in the previous subsection is shown in Figure 3a. The range was chosen comparable to that by Saha et al. [16] and the effect of the relaxation time scale parameter can be clearly seen. The larger the relaxation time parameter, the closer are the results to the full equilibrium solution. Even though the effect of the relaxation time parameter is large for the shock tube case, the question of what the physically correct solution is remains. Since it is not possible to answer that question due to the lack of experimental data, it is not possible to give the HRM nor the HEM an edge over the other. Instead, the sensitivity with respect to the relaxation time scale parameter on the results for a more realistic dodecane 2D test case representing typical gasoline direct injection (GDI) conditions as given in Bode et al. [2] is studied here. Results of this test case during early time steps, which should be more sensitive to the relaxation time parameter than time steps during steady-state, are shown in Figure 3b and Figure 3c. It can be seen that vapor is formed at the nozzle inlet edge, which moves towards the orifice. Since the orifice is still locked by liquid, non-condensable gases from outside have not penetrated into the nozzle yet and hydraulic flip has not occurred. Comparing both plots, the differences in the gas volume fraction inside the nozzle are negligible. This was also found to be true for all values of $C = [0.01, 100]$ considered here. Thus, the application of the developed 3-equation HEM for complex nozzle simulations seems reasonable.

Besides the simple usage of the developed 3-equation HEM due to its compatibility with single-phase solvers, the computational cost is another advantage. For the shown 2D test case, the computational cost of the 3-equation HEM simulations was about 46% smaller than that of the 5-equation model.

## Conclusions

A 3-equation HEM is presented in this work. It was developed for injector flows with non-condensable gases and allows arbitrary combinations of EOSs, which was shown to be important. Improvements of the convexification step and a novel tabulation method in the framework of HEM were summarized. Optimizations with respect to computational

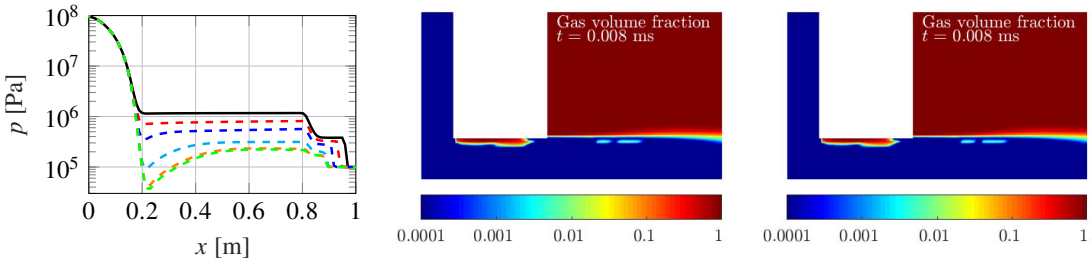


(a) Shock tube (b) 3-eq.: HEM (c) 5-eq.: HRM $\theta_0$

Figure 3: Shock tube results at $t = 0.473$ ms computed with the 5-equation model with infinitely fast relaxation (black, solid line) and various chemical relaxation time scales $C\theta_0$: red - $C = 100$, blue - $C = 10$, cyan - $C = 1$, orange - $C = 0.1$, green - $C = 0.01$, all dotted (left plot). Gas vapor fraction results of the 2D test case with a nozzle height of 0.065 mm and a nozzle length of 0.140 mm computed with the 3-equation HEM and a 5-equation HRM with $\theta_0$ using structured, uniform meshes at dimensionless time $t = 0.008$ (two right plots).

cost were explained. The HEM was found to match results of a 5-equation model with full relaxation and phase change and the reasonability of the equilibrium assumption was shown in the context of a GDI test case.

## Acknowledgements

The authors gratefully acknowledge funding by the Cluster of Excellence “Tailor-Made Fuels from Biomass” and Honda R&D.

## References

[1] M. Battistoni, D. Duke, A. B. Swantek, F. Z. Tilocco, C. F. Powell, S. Som, Effects of noncondensable gas on cavitating nozzles, Atomization and Sprays 25 (6) (2015) 453–483.
[2] M. Bode, T. Falkenstein, M. Davidovic, H. Pitsch, H. Taniguchi, K. Murayama, T. Arima, S. Moon, J. Wang, A. Arioka, Effects of cavitation and hydraulic flip in 3-hole gdi injectors, SAE International Journal of Fuels and Lubricants 10 (2) (2017) 380–393.
[3] R. Saurel, F. Petitpas, R. Abgrall, Modelling phase transition in metastable liquids: application to cavitating and flashing flows, Journal of Fluid Mechanics 607 (2008) 313–350.
[4] R. Saurel, F. Petitpas, R. A. Berry, Simple and efficient relaxation methods for interfaces separating compressible fluids, cavitating flows and shocks in multiphase mixtures, Journal of Computational Physics 228 (2009) 1678–1712.
[5] A. Zein, M. Hantke, G. Warnecke, Modeling phase transition for compressible two-phase flows applied to metastable liquids, Journal of Computational Physics 229 (8) (2010) 2964–2998.
[6] Y. Wang, L. Qiu, R. D. Reitz, R. Diwakar, Simulating cavitating liquid jets using a compressible and equilibrium two-phase flow solver, International Journal of Multiphase Flow 63 (2014) 52–67.
[7] M. Pelanti, K.-M. Shyue, A mixture-energy-consistent six-equation two-phase numerical model for fluids with interfaces, cavitation and evaporation waves, Journal of Computational Physics 259 (2014) 331–357.
[8] M. Bode, F. vom Lehn, H. Pitsch, Numerical investigation of the effect of dissolved non-condensable gases on hydraulic flip in cavitating nozzles, in: 10th International Cavitation Symposium, Baltimore, USA, 2018.
[9] A. Voss, W. Dahmen, Exact riemann solution for the euler equations with nonconvex and nonsmooth equation of state, Tech. rep., Fakultät für Mathematik, Informatik und Naturwissenschaften (2005).
[10] P. Helluy, H. Mathis, Pressure laws and fast legendre transform, Mathematical Models and Methods in Applied Sciences 21 (04) (2011) 745–775.
[11] O. Le Métayer, J. Massoni, R. Saurel, Élaboration des lois d’état d’un liquide et de sa vapeur pour les modèles d’écoulements diphasiques, International journal of thermal sciences 43 (3) (2004) 265–276.
[12] O. Le Métayer, R. Saurel, The noble-abel stiffened-gas equation of state, Physics of Fluids 28 (4) (2016) 046102.
[13] P. Downar-Zapolski, Z. Bilicki, L. Bolle, J. Franco, The non-equilibrium relaxation model for one-dimensional flashing liquid flow, International Journal of Multiphase Flow 22 (3) (1996) 473–483.
[14] D. P. Schmidt, S. Gopalakrishnan, H. Jasak, Multi-dimensional simulation of thermal non-equilibrium channel flow, International Journal of Multiphase Flow 36 (2010) 284–292.
[15] D. Duke, A. Swantek, Z. Tilocco, A. Kastengren, K. Fezzaa, K. Neroorkar, M. Moulai, C. Powell, D. Schmidt, X-ray imaging of cavitation in diesel injectors, SAE International Journal of Engines 7 (2) (2014) 1003–1016.
[16] K. Saha, S. Som, M. Battistoni, Investigation of homogeneous relaxation model parameters and their implications for gasoline injectors, Atomization and Sprays 27 (4) (2017) 345–365.